A&A 370, 586–590 (2001)
DOI: 10.1051/0004-6361:20010274

Astronomy & Astrophysics

Scatter broadening of pulsars in the direction of the Gum nebula

D. Mitra[1,⋆] and R. Ramachandran[2]

[1] Raman Research Institute, Bangalore 560 080, India
e-mail: dmitra@iucaa.ernet.in
[2] Stichting ASTRON, Postbus 2, 7990 AA Dwingeloo, The Netherlands

Received 24 November 2000 / Accepted 7 February 2001

Abstract. We have measured the scatter broadening of pulsars in the direction of the Gum nebula. For the first time, our observations show clear variations of scattering properties across the Gum nebula. The IRAS-Vela shell is shown to be a high scattering region. Our revised estimations of distances to these pulsars are consistently less by a factor of 2–3, which has very important consequences for the deduced values of radio luminosity and transverse velocity of pulsars.

Key words. ISM: Gum nebula – stars: pulsars: general

1. Introduction

The Gum nebula (first observed by Gum 1952, 1956) has the most extended Hα emission observed in the sky. The nebula extends for about 40° in angular size centered around galactic longitude $l \sim 255°$ and galactic latitude $b \sim -2°$. The distance to the nebula is found to be approximately ∼400 pc. Since the discovery of the Gum nebula its origin has been an extremely controversial topic which still has not been resolved. There are several theories for the nature of the Gum nebula and we briefly mention a few here. For a detailed review of the Gum Nebula see Bruhweiler et al. (1983).

The Gum Nebula appears extremely diffuse and faint in Hα thus making it extremely difficult to estimate its size. One of the earliest measurements gave its size to be as large as $75° \times 45°$ (Brandt et al. 1971). Refined estimates of the size of the nebula using wide field Hα imaging is given by Sivan (1974), which restricts the size to ∼36°. Based on a spectroscopic study of ionized gas, Reynolds (1976a,b) proposed that the Nebula is a one million year old expanding gas shell, originally produced by a supernova explosion, which is now being heated and ionized by the massive stars ζ Puppis and γ^2 Velorum. According to Reynolds, the average density of the nebula is as large as about 2 cm^{-3}. Assuming a diameter of about 250 pc, we can see that the nebula can potentially introduce a dispersion measure of about 500 $\mathrm{pc\,cm}^{-3}$.

According to Weaver et al. (1977), the stellar wind from ζ Puppis could be strong enough to produce the observed Nebula, which is a shell. The shell is formed by the interaction of the stellar winds from ζ Puppis and γ^2 Velorum with the ambient interstellar medium. They also predict soft X-rays from the hot interior, which is at a temperature of about 10^6 K. Wallerstein et al. (1980), from a study of the interstellar gas towards stars in the direction of the nebula, came to the conclusion that the nebula is consistent with a model of the Gum Nebula as an HII region ionized by OB stars and stirred up by multiple stellar winds. Chanot & Sivan (1983), on the basis of 60°-field Hα photographs, suggested that the Gum Nebula is composed of two regions, one which is a circular main body with a typical ring-like appearance of diameter of 36°, and the other which consists of faint diffuse and filamentary extensions which merge with the faint Hα background. This idea supports the model of Reynolds (1976a) for an expanding Hα shell ionized by UV flux of ζ Puppis and γ^2 Velorum. The origin of the shell structure is, however, uncertain.

From a detailed study of the Gum Nebula, Sahu (1992) came to the conclusion that the nebula is a shell-like structure surrounding the Vela R2 association which is at a distance of about 800 pc, while the shell-like structure near the Vela OB2 association known as the IRAS Vela shell is at a distance of about 450 Kpc. This hypothesis crucially depended on the distance to ζ Puppis, as this star is believed to be the primary source of ionization of the Gum Nebula, which Sahu (1992) found to be ∼800 pc. However the Hipparcos distance estimates to ζ Puppis rules out the above scenario. Rajagopal (1999) showed from the kinematics of the IRAS Vela shell that the Gum Nebula is either inside or overlapping with the shell.

The various possible alternative scenarios as discussed above has left several open ends in our understanding of the Gum Nebula. The electron density estimates inside the Gum Nebula, as shown by Reynolds (1976a),

Send offprint requests to: R. Ramachandran,
e-mail: ramach@astro.uva.nl
⋆ *Present address:* Inter University Center for Astronomy & Astrophysics, Post Bag 4 Ganeshkhind, Pune 411 007, India.

and Wallerstein et al. (1980), show large variations from 0.1 to 100 cm^{-3}. The complicated structure of the nebula is also evident from the Hα images available (e.g. Chanot & Sivan 1983).

Taylor & Cordes (1993, hereafter TC93), as part of their galactic free electron density distribution model, considered the Gum nebula as a separate component, with an angular diameter of 30 degrees. They assumed that the number density of free electrons is uniform all over this component (0.2 cm^{-3}). They also assumed that the fluctuation parameter, which determines the amount of scattering introduced by the medium, is zero. Though this is a drastic assumption (as, for example, demonstrated by the scattering properties of the Vela pulsar), as they state, this is mainly due to very poor constraints available. In this work, we have done a systematic survey across the Gum Nebula to measure the scatter broadening of pulsars due to the electron density fluctuations, which should eventually help to model the scattering properties of this region in more detail.

2. Sample selection and observation

We have observed 40 pulsars located in the galactic coordinate range $250° < l < 290°$ and $-20° < b < 20°$ with the Ooty Radio Telescope during March 1997. The Ooty Radio Telescope is a semi-parabolic cylinderical array, whose dimensions are about 500 m in North-South, and 30 m in East-West. It operates at a fixed centre frequency of 327 MHz. It has 1056 dipoles arranged North-South along the focal line of the semi parabolic cylinder, and as the result of which it is not sensitive to the other (East-West) component of polarization (for further details refer Swarup et al. 1971; Sarma et al. 1975a, 1975b; Kapahi et al. 1975).

Although there are in total 48 known pulsars in this range, we selected only those above a flux (at 400 MHz) of 5 mJy. The dispersion measures (DM) of these pulsars are in the range 30–306 pc cm^{-3}. Our sample also includes pulsars for which scatter broadening measurements at other frequencies exist in the literature.

To carry out these observations, we have used a pulsar receiver that was mainly built for pulsar searches (Ramkumar et al. 1994). The pulsar receiver consists of a 4-bit sampler (Analog-to-digital converter), which samples the incoming signal voltage of bandwidth 8 MHz. The output of this is fed to an FFT engine. The FFT produces 256-point complex spectra which are converted to power spectra using look-up tables. The resultant power spectra are pre-integrated over successive spans of ∼0.5 msec, which is the final time resolution in recorded data. A block integration is done over a number of pre-integrated samples for calculation of the running mean for each of the 256 frequency channels. The running mean is finally subtracted from the pre-integrated data to remove the effects of receiver gain variations. The mean subtracted pre-integrated data are then represented as a one-bit signal by recording the sign bit and stored on magnetic tape.

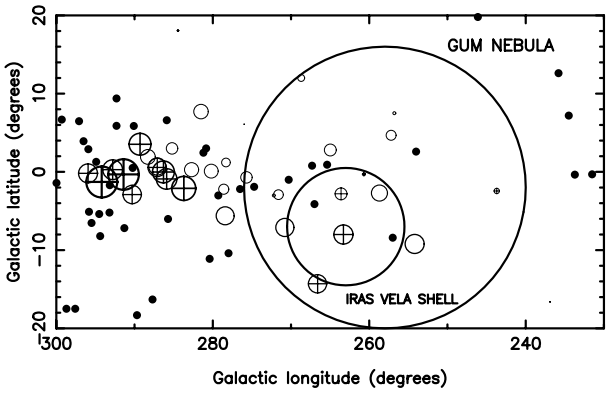

Fig. 1. Observed scatter broadening (τ_{sc}) of pulsars at 327 MHz plotted as a function of the galactic coordinates. The circles with crosses correspond to pulsars for which earlier τ_{sc} measurements are available. The open circles are the pulsars observed using the ORT. Size of these symbols is proportional to $\log(\tau_{sc})$, where τ_{sc} is in milliseconds. Pulsars indicated as "dots" are those for which the scatter broadening measurements are not available. The Gum nebula is indicated by the larger circle with radius of ∼18° with morphological center at $l = 258°$ and $b = -2°$. The smaller circle indicates the IRAS-Vela shell, with a radius of ∼7.5°, with centre at $l = 263°$ and $b = -7°$ (adopted from Sahu 1992). Our sample consists also of pulsars outside the "main body" of the Gum Nebula (Chanot & Sivan 1983), as it is possible that the faint diffuse and filamentary extensions are possibly part of the nebula itself

We observed each pulsar for 20 min, and compensated for the interstellar dispersion by offline analysis. The integrated pulse profiles were obtained by folding the time series with the correct rotation period of the pulsar.

2.1. Measurement of scatter broadening

Out of the 40 pulsars in our sample, only 21 were above our detection limit. For each observed pulsar, we compensate for the interstellar dispersion by offline software, and fold the time series with the exact expected rotation period, to produce average pulse profiles.

The scatter broadening was then estimated by a least-square-fit to the average pulse profile with the following model: the observed pulse profile function $P(t)$ is the convolution of the intrinsic pulse profile (which is emitted by the pulsar) $P_i(t)$ with (1) the impulse response characterising the scatter broadening in the ISM $T(t)$, (2) the dispersion smearing function across the spectral channel in the receiver $S(t)$, and (3) the instrumental response function $I(t)$.

$$P(t) = P_i(t) \otimes T(t) \otimes S(t) \otimes I(t) \quad (1)$$

where $\otimes$ denotes convolution. In a simple picture, where the scattering material is assumed to be concentrated in a region whose thickness is very small when compared to the distance between the observer and the pulsar, the impulse response function is $T(t) = \exp(-t/\tau_{sc})$. The whole procedure we have adopted to compute this τ_{sc} is described in detail in Ramachandran et al. (1997).

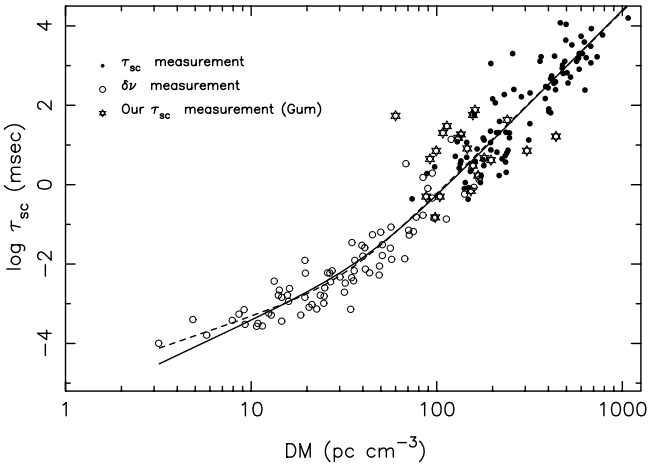

Fig. 2. A plot of $\tau_{\rm sc}$ vs. DM for 188 pulsars. The $\tau_{\rm sc}$ values have been scaled to 400 MHz. Stars in the plot represent our $\tau_{\rm sc}$ measurements given in Table 1. Open circles are from the decorrelation band width measurements, using the relation $2\pi\nu\tau_{\rm sc} = 1$. Filled circles are the directly measured $\tau_{\rm sc}$ values. The values of the open and filled circles are taken from the Princeton pulsar catalogue (Taylor et al. 1993) and Ramachandran et al. (1997). The best fit models are plotted as lines. See text for details

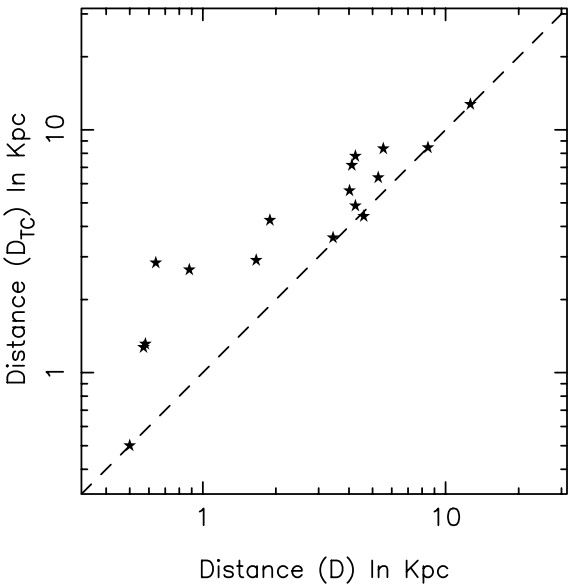

Fig. 3. A comparison between the distance $D_{\rm TC}$ obtained from the TC93 model and the distance (D) calculated using our method is shown by the star symbol in the above figure. The dashed line correspond to the case $D = D_{\rm TC}$. Note that for most of the cases the model distances are overestimated (see text for more details)

The results of the fit are given in Table 1. In Table 1, PSRs J0742–2822, J0745–5351 and J0835–4510 were not observed by us; we have used the scattering measurements listed in the literature (Roberts & Ables 1982; Alukar et al. 1986). For those measurements not done at 327 MHz, we have used the frequency scaling law $\tau_{\rm sc} \propto \nu^{-4.4}$ (where ν is the observing frequency) to obtain the scatter broadening value at 327 MHz. PSRs J0809–4753, J0837–4145 and J0840–5332 in Table 1 have had their scatter broadening reported earlier at frequencies other than 327 MHz, but we have reobserved them. The values listed for them in the table are from our measurements.

Figure 1 gives the spatial distribution of the pulsars across the Gum nebula as a function of the galactic coordinates. Note that the distribution is skewed to one side (mostly lying in the longitude range of 255° to 275°) of the nebula marked by the large circle in the figure. This must be primarily due to the fact that pulsars are mostly concentrated in the galactic disk and at such galactic longitudes toward the Galactic anti-center one does have significant contribution from the disk. Pulsars with high $\tau_{\rm sc}$ appear to lie behind the IRAS vela shell, as marked by the small circle in the figure.

3. Discussion

In Fig. 2 we plotted the values of scatter broadening $\tau_{\rm sc}$ for the whole pulsar population including our new results as a function of dispersion measure (DM). A function of the form as given by $\tau_{\rm sc} = A\ DM^{\alpha}\ (1 + B\ DM^{\gamma})\lambda^{4.4}$ msec, as discussed by Ramachandran et al. (1997), is shown as a fit to the data points, where λ is the wavelength in meters. On inclusion of our new measurements the fit does not seem to change significantly. The dotted curve in the figure corresponds to $A = 4.5\ 10^{-5}$, $B = 3.1\ 10^{-5}$, $\alpha = 1.6$, $\gamma = 3$. The solid curve is modelled by fixing $\alpha = 2.2$ which is the expected dependence from Kolmogorov spectrum, thus giving $A = 8.4\ 10^{-6}$, $B = 8.3\ 10^{-5}$ and $\gamma = 2.5$. The term $(1 + B\ DM^{\gamma})$ should provide a useful description of the apparent mean dependence of the turbulence level on DM. The scatter around the mean trend may be understood as due to possible existance of isolated regions of enhanced scattering in the line of sight, and consequent failure of the assumption that the scatterer is half way down the line of sight.

Though PSR J0924–5814 seems to have a large deviation compared to the mean Kolmogorov line, the error in the estimate of $\tau_{\rm sc}$ for this pulsar is more than 100% (refer Table 1) due to poor signal-to-noise ratio of the integrated pulse profile.

The presence of the Gum nebula has been invoked explicitly in models estimating pulsar distances and free electron density distribution in the Galaxy (e.g. Bhattacharya et al. 1992, TC93 and references therein). TC93 modelled the Gum nebula as a sphere of 130 pc radius at a distance of 500 pc, with a uniform electron density of 0.25 cm^{-3}, and the density falls off as an one-sided Gaussian with an rms of 50 pc. They also assumed that the fluctuation parameter, which is defined as

$$F = \frac{\zeta\epsilon^2}{\eta}\left(\frac{l}{1\ \rm pc}\right)^{-2/3}, \qquad (2)$$

is zero. Here, ζ is the normalised variance of large-scale electron density fluctuations, ϵ^2 is the corresponding quantity for small-scale density variations, η the volume filling factor for ionised regions, and l the outer scale limit

Table 1. Summary of the measured scattering properties. Columns 1–10 indicate (1) Pulsar name, (2) DM, (3) measured scatter broadening, $\tau_{\rm sc}$, (4) intrinsic width, $w_{\rm i}$ (5) error in $(\tau_{\rm sc} + w_{\rm i})$, (6) number of degrees of freedom, (7) normalised χ^2 values, (8) fluctuation parameter, (9) derived distance, and (10) distance given by TC93 model. [1]Those for which $\tau_{\rm sc}$ values are obtained from earlier measurements: these were not observed by us. [2]Those for which $\tau_{\rm sc}$ earlier measured values are available, but have also been reobserved by us. [†]Those for which proper motion measurements are already available

Name	DM (pc cm^{-3})	$\tau_{\rm sc}$ (msec)	$w_{\rm i}$ (msec)	$\Delta(\tau_{\rm sc} + w_{\rm i})$ (msec)	$N_{\rm dof}$	χ^2	F	Distance (kpc)	$D_{\rm TC}$ (kpc)
†J0738–4042	160.8	76 ± 3					6.3	4.5	>11.03
†J0742–2822[1]	73.7	1					0.8	0.65	1.89
J0745–5351[1]	122.3	60					7.0	4.11	>7.14
J0809–4753[2]	228.3	79 ± 18	9 ± 10	8	697	1.03	5.9	>12.65	>12.72
J0820–4114	113.4	30 ± 11	42 ± 14	9	216	1.23	6.6	0.64	2.83
†J0835–4510[1]	68.2	8					6.3	0.50	0.50
J0837–4135[2]	147.6	1 ± 1	9 ± 3	2	597	3	0.0	1.89	4.24
J0840–5332[2]	156.5	57 ± 11	13 ± 10	10	218	1.1	5.3	4.25	7.78
J0846–3533	91.1	4 ± 5	44 ± 6	5	135	2.1	1.7	0.58	1.31
J0855–3331	87.7	1 ± 3	24 ± 1.5	1	595	1.3	0.0	0.57	1.27
J0904–4246	189	8 ± 4	21 ± 4	3	397	0.99	0.8	4.6	4.40
J0905–5127	189	4 ± 7	11 ± 8	5	218	0.88	0.5	5.54	8.35
J0907–5157	104	1 ± 13	32 ± 10	10	228	0.9	0.15	0.88	2.65
J0924–5302	152.9	1 ± 1	6 ± 0.8	1	195	1.1	0.15	4.02	5.61
J0924–5814	60.0	55 ± 65	1 ± 50	45	238	1.0			2.01
J0934–5249	99.4	7 ± 13	21 ± 10	5	197	1.1	1.3	1.66	2.90
J0942–5552	180.2	5 ± 1.5	7 ± 2	2	237	1.1	0.3	5.28	6.35
J0952–3839	167	2 ± 12	48 ± 10	8	227	0.91	0.25	>8.46	>8.44
J0955–5304	156.9	3 ± 1	5 ± 1	1	122	1.2	0.67	4.25	4.86
J1001–5507	130.6	15 ± 2	13 ± 2	2	197	1.1	10.7	3.44	3.59
J1003–4747	98.1	0 ± 4	9 ± 4	3	197	1.2			3.44
J1017–5621	439.1	16 ± 36	8 ± 25	25	228	0.97			11.77
J1042–5521	306	7 ± 10	29 ± 10	10	238	1.1			6.95
J1046–5813	240.2	43 ± 50	2 ± 50	50	238	1.03			4.8
J1059–5742	107.9	2 ± 3	20 ± 7	5	237	1.2			2.74

for an assumed Kolmogorov power law of the density turbulence of free electrons. The assumption that F is zero means that the nebula contributes to dispersion measure, but not to the scattering properties. As the authors state, this is mainly due to the very poor knowledge of the scattering properties of pulsars in that direction.

From our observation, it is obvious that many parts of the nebula significantly contribute to enhanced scattering of pulsar signals. This issue was addressed by Deshpande & Ramachandran (1998) in detail, where they explicitly showed that in order to explain the enhanced scattering observed for PSR J0738–4042, which is a pulsar in the Gum Nebula (refer Table 1), one has to increase $n_{\rm e}$, and adopt values of fluctuation parameter almost equal to that of the spiral arm. We have used a similar method as suggested by Deshpande & Ramachandran (1998), and have obtained the distances and the fluctuation parameters for the pulsars behind the Gum Nebula under the framework of the TC93 model. which we briefly describe below.

Deshpande & Ramachandran (1998) showed that if the distance to a dominant discrete scatterer is known, then it is possible to use only the DM and the $\tau_{\rm sc}$ measurements to constrain F and distances to pulsars lying behind the scattering region. With the available data on the Vela pulsar and J0738–4042, they find similar values of $n_{\rm e}$ and F, of about 0.32 cm^{-3} and 6.3, respectively. This helped constrain the distance of J0738–4042 to 4.5 kpc (as opposed to >11 kpc by TC93). As they suggest, it seems reasonable to characterise a major part of the Gum nebula with $n_{\rm e} = 0.32$ cm^{-3} and a fluctuation parameter $F = 6.3$. In a simple exercise, for various lines-of-sight in the Gum Nebula we have applied the above technique to obtain F and distances to pulsars, keeping $n_{\rm e}$ fixed at 0.32. The values of F and distances (in kpc) obtained is given in Table 1. Though these values are not unique (as different

combinations of n_e and F can match the observed values of DM and τ_{sc}), as Deshpande & Ramachandran (1997) show, it is not unreasonable. It is interesting to note that most of the pulsars lying in the IRAS Vela shell seems to be consistent with a fluctuation parameter of ∼6.5, while the other regions in the Gum Nebula have an F of only ∼0.5. This, at least intuitively, indicates that the IRAS-Vela shell is a different entity with different fluctuation properties. Note that we have not attempted any modelling of the region outside the Gum Nebula. The value of F for PSR J1001–5507 is 10.7, which we believe is too high to be associated with the nebula. For PSR J0924–5814, we get a value of 25 which is unreasonable, and this is due to the poor estimation of τ_{sc}. Thus, we reject this pulsar in our analysis.

The distances we obtain from our procedure seem to be consistently different from the values obtained by the TC93 model (as shown in Fig. 3). It is worth noting that out of this list in the table, proper motion measurements are already available for those pulsars marked with a dagger (†). For them, on the average, our analysis makes a difference of 2–3 in the estimated value of transverse velocity.

As an extension of the present study to a more detailed one, it would be interesting to establish the electron density variation of the Gum Nebula along the various lines-of-sight of these pulsars. As found by Reynolds (1976b), the number density in the Gum nebula can in principle vary by many times, with an average density of about 2 cm^{-3}. This can potentially introduce dispersion measures of the order of 500 $pc\,cm^{-3}$. Estimates of density variations can be obtained from detailed Hα studies, which involves measuring emission measures in the line-of-sight to pulsars. The ratio of the emission measure and the DM can be used to estimate the electron densities. Although such estimates are available (Reynolds 1976a), they are not sufficient for the entire set of lines-of-sight observed. Further, as we have estimated the scatter broadening of only a subset of pulsars in this region, there remains a significant fraction of pulsars for which such measurements are not available (as clearly seen in Fig. 1). With a more sensitive instrument, it should be possible to enlarge the sample of scatter broadening measurements, giving further clues about the electron density distribution.

Acknowledgements. We would like to thank Dr. A. A. Deshpande of the Raman Research Institute for his invaluable help and stimulating discussions. We would also like to thank V. Balasubramanium for providing us with telescope time and help during the observations in Ooty. We would like to thank Bilal and Mangesh for their kind help during the observations.

References

Alurkar, S. K., Slee, O. B., & Bobra, A. D. 1986, AJP, 39, 433
Bhattacharya, D., Wijers, R. A. M. J., Hartman, J. W., & Verbunt, F. 1992, A&A, 254, 198
Brandt, J. C., Stecher, T. P., Crawford, D. L., & Maran, S. P. 1971, ApJL, 163, L99
Bruhweiler, F. C., Kafatos, M., & Brandt, J. C. 1983, Comments on Modern Physics, Part C – Comments on Astrophysics (ISSN 0146-2970), 10, 1
Chanot, A., & Sivan, J. P. 1983, A&A, 121, 19
Deshpande, A. A., & Ramachandran, R. 1998, MNRAS, 300, 577
Gum, C. S. 1952, Observatory, 72, 151
Gum, C. S. 1956, Observatory, 76, 150
Gwinn, C. R., Bartel, N., & Cordes, J. M. 1993, ApJ, 410, 673
Kapahi, V. M., Damle, S. H., Balasubramanian, V., & Swarup, G. 1975, J. IETE, 21, 117
Ramkumar, P. S., Prabu, T., Girimaji, Madhu, & Markandeyulu, G. 1994, JApA, 15, 343
Rajagopal, J. 1999, Ph.D. Thesis, Raman Research Institute, Bangalore
Reynolds, R. J. 1976a, ApJ, 203, 151
Reynolds, R. J. 1976b, ApJ, 206, 679
Roberts, J. A., & Ables, J. A. 1982, MNRAS, 201, 1119
Ramachandran, R., Mitra, D., Deshpande, A. A., McConnell, D. M., & Ables, J. G. 1997, MNRAS, 290, 260
Sivan, J. P. 1974, A&AS, 16, 163
Sahu, M. S. 1992, Ph.D. Thesis, University of Groningen
Sarma, N. V. G., Joshi, M. N., & Ananthakrishnan, S. 1975b, J. IETE, 21, 107
Swarup, G., Sarma, N. V. G., Joshi, M. N., et al. 1971, Nat. Phys. Sci., 230, 185
Sarma, N. V. G., Joshi, M. N., Bagri, D. S., & Ananthakrishnan, S. 1975a, J. IETE, 21, 110
Taylor, J. H., & Cordes, J. M. 1993, ApJ, 411, 674
Taylor, J. H., Manchester, R. N., & Lyne, A. G. 1993, ApJS, 88, 529
Wallerstein, G., Silk, J., & Jenkins, E. B. 1980, ApJ, 240, 834
Weaver, R., McCray, C. T., Castor, J., Shapiro, P., & Moore, R. 1977, ApJ, 218, 377